Article D

Títol: Hydrogen-bonded nanoporous frameworks with magnetic properties based on polycarboxylic polychlorinated triphenylmethyl radicals.

Autors: D. Maspoch, D. Ruiz-Molina, K. Wurst, N. Domingo, G. Vaughan, J. Tejada, C. Rovira, J. Veciana.

Publicació: En preparació.

(No presentat a la Comissió de Doctorat).

Hydrogen-Bonded Nanoporous Frameworks with Magnetic Properties based on Polycarboxylic Polychlorinated Triphenylmethyl Radicals

Daniel Maspoch,[†] *Daniel Ruiz-Molina,*[†] *Klaus Wurst,*[‡] *Neus Domingo,*[§] *Gavin Vaughan,* [℘] *Javier Tejada,*[§] *Concepció Rovira,*[†] *Jaume Veciana .* [†,*]

Contribution from the Institut de Ciència de Materials de Barcelona, CSIC, Campus Universitari de Bellaterra 08193, Cerdanyola, Spain, Institute für Allgemeine, Anorganische und Theoretische Chemie, Universität Innsbruck, Innrain 52ª, A-6020, Innsbruck, Austria, Facultat de Física, Universitat de Barcelona, Diagonal 647, 08028, Barcelona, Spain, European Syncrotron Radiation Facility (E.S.R.F.), B. P. 220, F - 38043 Grenoble cedex, France.

E-mail: vecianaj@icmab.es

RECEIVED DATE (to be automatically inserted after your manuscript is accepted if required according to the journal that you are submitting your paper to)

To whom correspondence should be addressed. Telephone: +34 93 5801853. Fax: +34 93 5805729.

† Institut de Ciència dels Materials de Barcelona.

‡ Universität Innsbruck.

§ Universitat de Barcelona.

℘European Synchroton Radiation Facility.

Introduction

In the last decade there has been increasing interest to control the intermolecular interactions and, therefore, the mutual orientation of the constituent organic open-shell synthons to design organic/molecular magnetic materials. The discovery of the first organic ferromagnet by Kinoshita et al,[1] the η form of the *p*-nitrophenyl nitronyl nitroxide (**1**) in 1991, that orders magnetically at 0.6 K opened new perspectives in this field. This fortuitous result stimulated the preparation of successive purely organic ferromagnets, which permitted obtaining several examples of aromatic derivatives of nitroxides and nitronyl nitroxides ferromagnets **2-11** (Scheme 1).[2,3] Although the majority order below 1 K, some exceptions include the neutral oligo-nitroxide radical **12** discovered by Tholance et al[4] that orders as a ferromagnet at 1.48 K and two radical cations salts, $[C_{60}][TDAE]$ (**13**) and $[BBDTA]GaCl_4$ (**14**) reported by Thompson et al.[5] and by Awaga et al.,[6] which order at 16 and 6.7 K, respectively. More recently, an interesting approach proposed by Rawson et al. and based on the supramolecular arrangement of thiazyl radicals has yield two new organic ferromagnets **15** and **16**, which order at 36 K as a weak ferromagnet and 1.32 K, respectively.[7]

However, even though these examples of organic/molecular ferromagnets have been reported, many difficulties have been appear to establish a methodology for an ultimate designing of organic ferromagnets. First, there is an intrinsic difficulty that exists for establishing ferromagnetic interactions between spins belonging to neighboring open-shell species, owing to the natural predilection for an antiparallel spin alignments in these molecules. Secondly, there are complications that usually arise when a transmission of such intermolecular ferromagnetic interactions, along three or two dimensions of the solid and over a long range, is desired. And thirdly, due to the fact of the impossibility to predict the ultimate structure of even the simplest crystalline solids from a knowledge of their chemical composition.[8]

- Insert Schart 1 -

In order to minimize these inconveniences, crystalline engineering tools are needed. Crystal engineering is the design, construction and study of crystal structures from molecular components built with intermolecular interactions.[9] Among the different supramolecular interactions that exist, hydrogen bonds have been studied in depth because their directional and often predictive nature may allow to control long-range supramolecular order in solid state.[10] Hydrogen bonds are formed by strong donor-acceptor functionalities (OH, NH_2, CO_2H, $CONH_2$) and with weak donors (C-C-H, C_6H_5, C=C-H, $C(sp^3)$-H) and acceptors (CN, NO_2, halogen, ϕ). In such a context, Veciana et al.[11] and Sugawara et al.[12] proposed the idea to use these hydrogen bonds to control the self-assembly of open-shell building blocks. Such a study was initiated by studying the family of aromatic derivatives nitronyl nitroxides with one or two hydroxylic groups on the aromatic ring as functional groups susceptible to form hydrogen bond interactions. Success of this approach was reflected in two different organic ferromagnets **17**[13] and **18**[14] substituted with one and two hydroxylic groups, which orders at 0.45 and 0.50 K, respectively. Moreover, additional examples belonging to this family have provided an interesting assortment of magnetic behavior.[15]

In addition to the hydroxylic groups, carboxylic groups are also important in the crystal engineering because they also form strong and directional O-H···O hydrogen bonds. H-bonded patterns in carboxylic in solid state have been described in detail by Leiserowitz et al.[16] The most frequent and dominant hydrogen-bonded motif is the syn-syn centrosymmetric dimer. Furthermore, other patterns in the form of infinite non-cyclic H-bonded catemer motifs and more rare cyclic trimeric and tetrameric motifs have been found.[17] However, a recent search in the Cambridge Structural Database (CSD, version 1.5 (2002)) has confirmed the presence of another cyclic motifs, an H-bonded square, formed by four carboxylic groups . A detail representation of all these cyclic H-bonded motifs are given in Scheme 1. Given this background, in our group we have initiated a new experimental approach based on the synthesis and study of organic/molecular magnetic materials based on the supramolecular arrangement of carboxylic-based open-shell tectons. To control long range packing, we have chosen perchlorinated triphenylmethyl radicals (PTM) properly functionalized with two (PTMDC, **20**) and three (PTMTC, **21**)

carboxylic groups in the *para*- positions of the aromatic rings (Scheme 3). PTM radicals, in addition to eminent thermal and chemical stabilities,[18] are bulky molecules minimizing additional through-space intermolecular magnetic interactions. Moreover, from a structural point of view, PTMDC and PTMTC radical can be considered an expanded version of isophtalic acid and trimesic acid,[19] respectively, where the benzene-1,3-diyil or the benzene-1,3,5-triyl unit has been replaced by an sp^2 hybridised carbon atom decorated with three perchlorophenyl rings substituted with carboxylic groups. Therefore, the related trigonal symmetries and functionalities of both organic radicals provides a typical template for getting cavities or channels and generate purely organic open-framework nanoporous structures, a major goal nowadays within the crystal engineering field.[20,21] However, in comparison with the existence of an extensive list of zeolite-like inorganic-organic hybrid open-frameworks materials,[22,23] only a few reported examples of porous structures build from pure organic molecules are stable even in absence of solvent guest molecules, mainly due to the weakness of the intermolecular non-coordinative supramolecular interactions. To our knowledge, the supramolecular arrangement of the natural product gossypol (**22**) discovered by Ibragimov et al.[24] generated the first robust channel-like organic H-bonded structure. Indeed, removal of the solvent molecules in **22** do not produce a collapse of the channels but slightly decrease their sizes. Scheme 4 shows two other organic tectons, the bisalcohol **23** and the octaamine **24** reported by Bishop et al.[25] and Wuest et al.,[26] which also formed robust H-bonded structures. More recently, a novel polymorph of the tris(o-phenylenedioxy)cyclophosphazene (**25**) reported by Sozzani et al.[27] was able to retain its crystal structure after desolvation. Interestingly, the empty structure of **25** can absorb xenon gas atoms.

- **Insert Schart 2-**
- **Insert Schart 3-**
- **Insert Schart 4-**
- **Insert Scheme 1 -**

Following a step-wise procedure, in a previous communication we studied the supramolecular arrangement of the monocarboxylic radical PTMMC (**19**).[28] In the solid state PTMMC formed hydrogen-bonded dimers that promoted the transmission of a weak ferromagnetic interaction. Moreover, such ferromagnetic interactions were disrupted by the incorporation of ethanol molecules between the dimers. Thus, considering this transmission of ferromagnetic interactions through H-bonded carboxylic groups, the dimensionality of the paramagnetic H-bonded network has been increased with the self-assembly of PTMDC and PTMTC radicals. Their crystalline packing creates a series of supramolecular materials, named as Purely Organic-Radical Open-Framework materials (POROF), that not only combines the presence of interesting magnetic properties, but also the formation of nanochannel-like structures without self-interpenetration. In such a context, an open-framework structure, named as POROF-1, exhibiting nanocavities and antiferromagnetic interactions has been obtained by the self-assembly of PTMDC. Furthermore, the crystal packing of PTMTC generates a second example of open-framework structure (POROF-2) that shows the presence of tubular hydrophilic channels and magnetic ordering. Additionally, as was also observed with PTMMC radical, the modification of solvent used in the crystallization process of PTMTC radicals originates solvent-induced polymorphism. Playing with a polar protic solvent, as water, there has been obtained a different H-bonded network of PTMTC radical, hereafter called η-phase, which show huge changes in its crystal structure and, consequently, in its magnetic properties.

Experimental Section

General Considerations. All solvents were reagent grade from SDS and were used as received and distilled otherwise indicated. All reagents, organic and inorganic, were of high purity grade and obtained from E. Merck, Fluka Chemie and Aldrich Chemical Co. Thin-layer chromatography (TLC) was performed on aluminium plates coated with Merck Silica gel 60. Elemental analyses were obtained in the Servei de Anàlisi de la Universitat Autònoma de Barcelona. The ^{1}H-NMR spectra were recorded on a Bruker ARX 250 spectrometer. FT-IR spectra were performed on a Perkin-Elmer Spectrum One

spectrometer. UV-Vis and near-IR were recorded using a VARIAN Cary 5 instrument. Electrochemical experiments were performed with an Electromat 2000 system (ISMP Technologies), using a platinum wire as working electrode and a saturated calomel electrode (SCE) as reference electrode. Anhydrous CH2Cl2 was freshly distilled over P2O5 under nitrogen. Commercial tetrabutylammonium hexafluorophosphate (Fluka, electrochemical grade) was used as the supporting electrolyte.

ζH-(heptadecachloro-4,4'-dimethyltriphenyl)methane (28). A mixture of **27** (3.00 g, 4.34 mmol), chloroform (40 ml) and aluminium chloride (0.70 g, 5.23 mmol) was heated at 150ºC for 7 hours in a glass pressure vessel. The mixture was then poured on the ice/1 normal hydrochloric acid (50 ml) and extracted with chloroform (2x100 ml). The organic mixture was washed with aqueous sodium hydrogen carbonate (100ml) and water (100ml) and the organic layer was evaporated in vacuo. The residue was purified by TLC (silica gel, hexane) giving 2.90 g of **28** (78% yield) as white powder. IR (KBr): 3040, 1540, 1367, 1344, 1299, 1274, 1225, 1139, 1024, 950, 923, 897, 839, 811, 778, 714, 697, 549, 519, 490. 1H NMR (250 MHz, CDCl3): ι 7.1 (s, 1 H, CH), 7. 7 (s, 2 H, CHCl2). Anal. Calcd. for C21H3Cl17: C 32.05, H 0.38; Found C 32.28, H 0.48. d

ζH-(tridecachlorotriphenyl)methane-4,4'-dicarboxylic acid (29). A mixture of **28** (0.750 g, 0.874 mmol) and 20% oleum (125 ml) was heated at 150ºC for 3 hours. The final deep blue solution was cooled and poured into cracked ice, and the collected solid was washed with water, dissolved in ether and extracted with aqueous sodium hydrogen carbonate (2x100ml). The aqueous layer was acidified with HCl and extracted with ether. The solid extracted was recrystallized from ether/hexane to give 0.208 g of diacid **29** (31% yield) as white powder.[30] d

ζH-(octadecachloro-4,4',4''-trimethyltriphenyl)methane (31). A mixture of **30** (1.70 g, 2.58 mmol), chloroform (30 ml) and aluminium chloride (0.40 g, 3.00 mmol) was heated at 160ºC for 8 hours in a glass pressure vessel. The mixture was then poured on the ice/1 normal hydrochloric acid (50 ml) and extracted with chloroform (2x50 ml). The organic mixture was washed with aqueous sodium hydrogen carbonate (100ml) and water (100ml). Immediately, the organic layer was filtered and the collected solid was washed with water and pentane to give 2.22 g of **31** (95% yield) as white powder. IR

(KBr): 3040, 1540, 1390, 1368, 1350, 1303, 1271, 1139, 775, 713, 692, 485. 1H NMR (250 MHz, CDCl3): ι 7.1 (s, 1 H, CH), 7. 7 (s, 3 H, CHCl2). Anal. Calcd. for C22H4Cl18: C 29.15, H 0.44; Found C 29.34, H 0.28.d

ζH-(dodedecachlorotriphenyl)methane-4,4',4''-tricarboxylic acid (32). A mixture of **31** (0.55 g, 0.61 mmol) and 20% oleum (100 ml) was heated at 150ºC for 12 hours. The final deep blue solution was cooled and poured into cracked ice, and the collected solid was washed with water, dissolved in ether and extracted with aqueous sodium hydrogen carbonate. The aqueous layer was acidified and extracted with ether. The solid extracted was recrystallized from ether/*n*-pentane to give 0.44 g of triacid **32** (92% yield) as white powder. IR (KBr): 3500-2500, 1721, 1556, 1331, 1300, 1274, 824, 795, 715, 664, 571, 472. 1H NMR (250 MHz, [D1]CHCl3): ι 7.1 (s, 1 H, CH). Anal. Calcd. for C22H4O6Cl12: C 33.46, H 0.51; Found C 33.13, H 0.63. d

(Dodecachloro-4,4',4''-tricarboxytriphenyl)methyl radical (21). A mixture of triacid **32** (0.25 g, 0.317 mmol) and powdered NaOH (0.7 g) was shaken for 72 hours in the dark with DMSO (30 ml). The mixture was filtered and immediately iodine was added (0.093 g, 0.36 mmol) into the resulting solution. The solution was left undisturbed in the dark for 30 minutes, it was washed with an aqueous solution of sodium hydrogen sulphite and it was treated with Et_2O. Radical **3** was extracted with aqueous sodium hydrogen carbonate, and such aqueous layer was acidified and extracted with Et_2O. The solid extracted was recrystallized from ether/*n*-pentane to give 0.21 g of radical triacid **21** (85% yield) as red powder. IR (KBr): 3500-2500, 1740, 1694, 1662, 1537, 1441, 1408, 1352, 1326, 1290, 1251, 1226, 1040, 931, 752, 722, 665, 574, 522, 462. Anal. Calcd. for C22H3O6Cl12 (POROF-2): C 33.50, H 0.38; Found C 33.65, H 0.32. Anal. Calcd. for C22H3O6Cl12•CHCl3•H2O (η-phase): C 29.83, H 0.65; Found C 30.52, H 0.61.d

EPR Measurements. EPR spectra were recorded on a Bruker ESP-300E spectrometer operating in the X-band (9.3 GHz). Signal-to-noise ratio was increased by accumulation of scans using the F/F lock accessory to guarantee a high-field reproducibility. Precautions to avoid undesirable spectral line broadening such as that arising from microwave power saturations and magnetic field over-modulation

were taken. To avoid dipolar broadening, the solutions were carefully degassed three times using vacuum cycles with pure Ar. The g values were determined against the DPPH standard (g=2.0030).

Magnetic Susceptibility Measurements. Direct current (dc) magnetic susceptibility measurements were carried out on a Quantum Design MPMS SQUID susceptometer with a 55 kG magnet and operating in the range of 4-320K. Background correction data were collected from magnetic susceptibility measurements on the holder capsules. Diamagnetic corrections estimated from the Pascal contents were applied to all data for determination of the molar paramagnetic susceptibilities of the compounds.

X-Ray Crystal and Molecular Structural Analyses. X-ray single-crystal diffraction data for POROF-1 and η-phase of PTMTC was collected on an Nonius KappaCCD diffractometer with an area detector and graphite-monochromized Mo-Kζ radiation. X-ray diffraction data for POROF-2 was collected on a Kuma KM-8 diffractometer with a CCD area detector and silicon-monochromized synchroton radiation (ς = 0.53378 Å). The structures were solved by direct methods (SHELXS-97)[29] and refined with full-matrix least squares procedures using the program SHELXL-97. All non-hydrogen atoms were refined anisotropic displacements parameters. All hydrogen atoms were placed in idealized positions, and no further refinement was applied. The structural conditions and structural details are listed in Table 1.

Results and discussion.

Synthesis. Polycarboxylic-based perchlorinated triphenylmethyl radicals PTMDC and PTMTC were synthesized as describe above. Although the synthesis of radical PTMDC was previously described,[30] a new simplest and shorter methodology has been employed (Scheme 2). PTMDC was prepared following a new four-step procedure, starting from compounds **26** and **27**.[31] Dichloromethyl groups were introduced by reacting **27** with anhydrous chloroform following a Friedel-Crafts reaction in a pressure reactor at 150ºC for 7 hours. The reaction of **28** with fuming sulphuric acid was undertaken at 150ºC for 3 hours. To our knowledge, this is the first time that a similar reaction has been described. At

high temperatures, 20% fuming sulphuric acid hydrolyzes and subsequently oxidizes the dichloromethyl groups to carboxylic groups to furnish diacid **29**. Finally, treatment of the hydrocarbon precursor **29** with sodium hydroxide in DMSO gave a red solution of the carbanion, which was oxidized to dicarboxylate radical in the presence of iodine and finally acidified with HCl to obtain radical PTMDC (**20**). [30]

- Insert Scheme 2 –

The preparation of radical PTMTC was carried out following a similar synthetic strategy, the four-steps procedure outlined in Scheme 3. Tris(2,3,4,5-tetraclorophenyl)methane **30** was synthesized according to the well-documented method found in the literature.[31] The three dichloromethyl groups were introduced by reacting **30** with dry chloroform following a Friedel-Crafts reaction under high pressure at 160ºC for 8 hours. As for PTMDC, the dichloromethyl groups were hydrolyzed and oxidized with 20% fuming sulphuric acid at 150ºC for 12 hours. Finally, treatment of **32** with sodium hydroxide in DMSO, iodine and HCl was allowed to synthesize PTMTC radical. Both radicals PTMDC and PTMTC were obtained as stable species in solution and in solid state and characterized by different techniques such as elemental analysis, ESI-TOF/MS, FT-IR and ESR spectroscopies.

- Insert Scheme 3 –

Crystallization and Molecular Structure of PTMDC and PTMTC. Crystallization by slow diffusion of a solution of hexane into a solution of PTMDC in dichloromethane gave red prism crystals of POROF-1. Crystallization by slow evaporation of a solution of hexane into a solution of PTMTC in dichloromethane gave red hexagonal plate crystals of POROF-2. Single crystals of POROF-2 were also obtained by a slow evaporation of a solution of PTMTC in dichloromethane and hexane in 2:1 ratio. Crystallization by slow diffusion of a solution of hexane into a solution of PTMTC in dichloromethane,

ether and water in 1:1:0.1 ratio gave red needle crystals of η-phase of PTMTC. The intensity data in the single X-ray diffraction experiments was collected from all these crystals. Crystallographic data are summarized in Table 1.

- Insert Table 1 -

Radicals PTMDC and PTMTC that form the crystal structures POROF-1 (trigonal, R-3), POROF-2 (trigonal, P-3c1) and η-phase (triclinic, P-1) adopt the typical propellerlike conformation usually found in this family of radicals (Figure 1), which is defined by the torsion angles with values in the range of 56-44 º between the mean planes of the three polychlorinated aromatic rings and that formed by the three bridgehead carbon atoms and the methyl one (Table 2).[32] For PTMDC, the values of the torsion angles amount 44, 45 and 49 º, whereas PTMTC in η-phase presents values of 45, 51 and 52 º. In POROF-2, the high molecular symmetry on the crystal lattice is reflected by the presence of a C3 symmetry axis that crosses through the central carbon (C8) of PTMTC. Thus, the three polychlorinated aromatic rings are identical with a torsion angle of 50º. The conformation of all carboxylic groups is found to be syn-planar.[16] As was previously observed for PTMMC, the plane of the carboxylic groups lies orthogonal to that of the aromatic ring (81 and 90 º for POROF-1, 87 º for POROF-2 and 88, 79 and 81º for η-phase) due to the great steric hindrance of the chlorine atoms in ortho positions with respect the carboxylic group.[33]

- **Insert Figure 1 –**
- **Insert Table 2 -**

Dimeric Hydrogen-Bonded Motif in PTMMC and PTMDC acids. Perchlorinated triphenylmethyl radical acids PTMMC and PTMDC adopt the normal syn-syn centrosymmetric dimer R^2_2 (8) (Table 3). Crystal structure of PTMMC radical was previously reported.[28] The dimer motif is formed by identical

PTMMC••••PTMMC pairs with distances O1••••O2 of 2.676 Å and angles O1-H1····O2 of 144º (Figure 2a). Additionally, two H-bondings between O2••••Cl12 with distances of 3.263 Å form a bifurcated H-bonded patter (Figure 2b). These may be taken along with the dimer, to originate one-dimensional H-bonded chains (Figure 2c). Further supramolecular interactions, in concrete two Cl••••Cl contacts per molecule, contribute to an additional stabilization of the H-bonded chains. In the overall structure, each chain is mutually stacked through ten Cl•••Cl contacts per PTMMC molecule along the three axis.

- Insert Table 3 -

Similarly, PTMDC radical in POROF-1 presents a centrosymmetric dimer with disordering in the carboxyl groups (Figure 2d). The O3••••O4 distances in the dimer are 2.677 Å and the O4-H4····O3 angles are 164º. In this case, the participation of four additional H-bondings between the carboxyl groups and chlorine atoms yields a dissimilar bifurcated H-bonded pattern (Figure 2e). Therefore, this conformation links each dimer motif with four PTMDC molecules through O····Cl H-bondings (O3····Cl11 3.092 Å and O4····Cl9 3.231 Å), extending the three-dimensionality of the H-bonded network. Effectively, considering the R^2_2 (8) dimers and O3····Cl11 H-bondings, a two-dimensional H-bonded sheet is formed along the *ab* plane (Figure 3a). In addition, taking into account the O4····Cl9 H-bondings, this complex H-bonded network is extended along the *c* axis (Figure 3b).

- **Insert Figure 2 –**

- **Insert Figure 3 –**

Hexameric Hydrogen-Bonded Motif in PTMDC and PTMTC acids. A recent search in the Cambridge Structural Database (CSD, version 1.5 (2002)) has been confirmed that the highest H-bonded cyclic motif found, formed by carboxylic groups, is the unusual tetrameric [R^4_4(16)] motif. For

this reason, there is surprising the ability of PTMDC and PTMTC radicals to arrange in a new hexameric [$R^6_6(24)$] motif. This new centrosymmetric motif is formed by six mutually H-bonded carboxylic groups of PTMDC and PTMTC radicals with O1···O2 distances of 2.692 and 2.657 Å, and O-H···O angles of 168.9 and 169.3 º, respectively.

- **Insert Figure 4 –**

Hydrogen-Bonded Network of POROF-1. The crystal of POROF-1 shows a two-dimensional porous H-bonded network containing large nanocavities. More in detail, molecular arrangement of PTMDC creates a primary structure consisting of two-dimensional H-bonded sheets along the *ab* plane, where each molecule of PTMDC adopts both H-bonded motifs, the dimeric [R_2^2 (8)] and the unusual hexameric [R_6^6 (24)] motifs. The repetitive unit consists in the hexameric [R_6^6 (24)] motif, which involves the participation of one of two carboxylic groups of PTMDC radical (Figure 4a). The second carboxylic group of each PTMDC radical forms the dimeric motif, which acts as a connecting element. Indeed, the formation of the dimer permits to connect each hexamer with six more identical units in an hexagonal topology, extending the infinitely H-bonded net along the *ab* plane (Figure 5).

The detailed packing structure is shown in Figure 6. Along the *c* axes, the crystal structure of POROF-1 reveals a supramolecular stacking of laterally shifted layers, yielding an ABCABC arrangement. The packing of these pillared sheets originates a pure organic open-framework structure with one-dimensional nanochannels formed by narrowed polar windows and larger hydrophobic cavities. These channels contain large hydrophobic supercages with dimensions of 10 Å in diameter, and smaller windows formed by each hexameric motif. As a consequence, a highly hydrophilic environment is presented due to the presence of the carboxylic groups at the inner walls. The diameter of such hydrophilic windows is 5 Ù considering van der Waals radius. The unusual combination of supercages and windows gives way to solvent-accessible voids in the crystal structure that amount up to 31% (5031 $Å^3$ per unit cell) of the total volume (16158 $Å^3$).

Further weaker supramolecular interactions, in concrete four H-bondings between chlorine atoms and carboxyl groups corresponding to the bifurcated pattern (Figure 2e) and several Cl···Cl contacts stabilize the overall structure. Among them, the two H-bondings involving O3····Cl11 atoms and six Cl···Cl contacts per molecule stabilize each H-bonded sheet, whereas the other two involving O4···Cl9 atoms and six Cl···Cl contacts per molecule link adjacent layers (Table 3).

- **Insert Figure 5 –**

Hydrogen-Bonded Network of POROF-2. When an additional carboxyl group is added in the perchlorinated triphenylmethyl skeleton, a substantial change in the arrangement of the radicals occurs: the dimeric motif as well as additional O····Cl H-bondings disappears from the crystal structure. Indeed, POROF-2 is exclusively constructed from the hexameric motif.

The crystals of POROF-2 show also a porous two-dimensional H-bonded structure, where each PTMTC radical participates in the formation of three identical H-bonded hexameric motifs. Topologically, each plane grows in an hexagonal form. Thus, each hexameric unit is H-bonded to six identical motifs along the *ab* plane (Figure 5). The packing of these H-bonded layers creates an open-framework structure. The pillared planes in an ABAB alternation along the *c* axis generates a three dimensional structure that exhibits tubular channels, where a sphere 5.2 Å in diameter can fit inside them (Figure 6). Indeed, the columnar disposition of H-bonded hexameric units originates highly hydrophilic tubular channels with a solvent-accessible voids that amount up to 15% (450 $Å^3$ per unit cell) of the total volume.

- **Insert Figure 6 –**

As occurs in POROF-1, the secondary crystalline structure can be defined as a three dimensional structure stabilizes by several weaker supramolecular interactions. However, no other H-bondings have

implications for the rigidity of this porous framework. In POROF-2, several chlorine-chlorine contacts – six per molecule- stabilize each H-bonded sheet, whereas also six Cl···Cl contacts per molecule link adjacent layers (Table 3).

Hydrogen-Bonded Network of η-phase of PTMTC. In contrast with the H-bonded hexameric motifs that molecules of PTMTC adopt in POROF-2, the repetitive unit in η-phase consists of a H-bonded trimer of radicals. Each trimer unit is formed by three carboxylic groups linked through two H-bonding (O3••••O2 and O5••••O4) with bond distances of 1.785 Å and 1.855 Å and angles of 170.69º and 174.30º, respectively (Figure 7a). Remarkably, the formation of hexameric unit in POROF-2 is prevented by the presence of solvent water molecules. The symmetry operation about *a* axes generates a supramolecular pattern composed of two H-bonded trimers strongly bonded to two water molecules through eight H-bondings (Figure 7b, Table 3). Therefore, this supramolecular association can be analyzed as an hexamer unit splited for two molecules of water, in where one of the two trimer units has been displace along the *b* axes, as shown Figure 8. Each water molecule participate in two hydrogen-bonding with two carboxylic groups of different trimers (O1••••O7 and O7••••O6) with distances of 1.631 Å and 2.187 Å and angles of 173.38º and 136.95º that connect both repetitive units. Simultaneously, both hydrogen atoms of each water molecule are also involved in two hydrogen-bonding with two carboxylic groups of a repetitive unit (O7••••O4 and O7••••O2) with bond distances of 2.320 Å and 2.315 Å and angles of 131.43 and 134.16º. Overall, the complex supramolecular pattern is composed of a total of 14 hydrogen bonds.

-Insert Figure 7 -

-Insert Figure 8 -

The long-range assembly of molecules of PTMTC thus formed can be considered as one-dimensional H-bonded chains of molecules of PTMTC that run along the *b* axes (Figure 7c). These chains are

connected to each other by water molecules to form a two-dimensional H-bonded sheet along the *bc* plane (Figure 9). Otherwise, the presence of several Cl····Cl contacts, as previously observed for the ζ-phase, also stabilizes the arrangement of PTMTC along the plane and the *c* axis (Table 3). In total, each molecule of PTMTC participates in six Cl····Cl contacts with distances of 3.33-3.57 Å. Finally, two H-bonding per molecule (O3····Cl6 3.273 Å) also connects adjacent planes along the *c* axes.

-Insert Figure 9 -

Structural rigidity of POROF-1 and POROF-2. The remarkable steric congestion originated by the large number of chlorine atoms present in the skeleton of polycarboxylic-based PTM radicals have significant implications for the structural properties of the open-framework structures POROF-1 and POROF-2 formed in the solid state since they contribute to: 1) increase the high thermal and chemical stability of each carboxylic-based PTM radical at a molecular scale, 2) induce the torsion in the phenyl rings, which defines their typical propellerlike conformation, 3) induce the orthogonallity of the carboxyl plane respect to that of the aromatic ring, 4) stabilize the crystal structures through the formation of multiple Cl····Cl contacts in the solid state; and 5) although Kitaigorodski's principle of close crystal packing indicates that organic synthons tend to interpenetrate, the remarkable steric congestions originated by the large number of bulky chlorine atoms, may be ascribed as the main reason for the obtaining of a noncatenated crystal packings.

Among them, in addition to the highly robust H-bonds, the formation of several Cl····Cl contacts in the solid state has significant contributions for the structural rigidity POROF-1 and POROF-2 networks. X-ray powder diffraction (XRPD) and thermal gravimetric studies shows that porous POROF-2 presents a highly structural rigidity in absence of solvent molecules. Single X-ray diffraction studies joined to thermal gravimetric experiments and elemental analysis confirm that POROF-2 crystallizes without guest solvent molecules (hexanes and/or methylene chloride) within the tubular nanochannels, which might be due to their highly polar environment (Figure 10a, Table 4). Thermogravimetric analysis of a

few single crystals of POROF-2 showed no weight loss in the temperature range of 25 to 285ºC. On the contrary, POROF-2 remains crystalline and stable up to 285ºC. Indeed, the XRPD pattern of a sample that was heated up to 285ºC shows that the positions and intensities of all lines remain unchanged when compared with the powder X-Ray diffraction pattern of an as-synthesized sample. Elemental analysis of this heated sample confirms no modification of the chemical composition (Table 4). A further increase of the temperature above 285ºC reveals a decomposition of POROF-2 as confirmed by combined powder X-ray diffraction and FT-IR characterization.

-Insert Figure 10 -

-Insert Table 4 -

A similar structural rigidity and integrity is shown in POROF-1 network. For POROF-1, thermal gravimetric analysis shows a weight loss of 9 % in the temperature range of 50-95 ºC (Figure 10b), ascribed to the complete loss of all guest *n*-hexanes molecules (in the as-synthesized material, the large hydrophobic cavities are occupied by six *n*-hexane solvate molecules (one molecule of *n*-hexane per one molecule of radical **1**). Such a loss was confirmed by complementary elemental analysis (Table 4). Beyond this temperature, thermal analysis does not exhibit any significant change up to 285 ºC, whereupon an abrupt weight loss attributed to the decomposition was observed. Simultaneously, XRPD studies confirmed that POROF-1 remains crystalline and stable up to 285 ºC. Indeed, the XRPD pattern of a sample that was heated at 265 ºC shows that the positions and intensities of all lines remain unchanged when compared with the XRPD pattern of an as-synthesized sample.

Magnetic Property of POROF-1, POROF-2 and η-phase PTMTC. Variable temperature magnetic susceptibility data for all crystalline samples of POROF-1, POROF-2 and η-phase PTMTC were obtained on a SQUID susceptometer, under a temperature range of 1.8-300 K. The θ•T values for the polycrystalline samples of POROF-1, POROF-2 and η-phase PTMTC are depicted in Figure 11. The

θ•T product value of the three samples at room temperature were 0.374, 0.384 and 0.360 emu·K·mol^{-1}, respectively. Since all these values are close to the theoretical value of 0.375 emu·K·mol-1 expected for an uncorrelated spins (S=1/2), the purity of the samples was assured. Furthermore, as the temperature decreases, the θ•T value remains constant for all the organic materials, showing a paramagnetic behavior in the 300-50 K temperature range. Below 50 K, magnetic measurements done in POROF-1 shows that θ•T value decreases upon decreasing temperature, consistently with the presence of weak intermolecular antiferromagnetic interactions. Identical measurements performed in POROF-2 shows that θ•T value remains constant down to 5 K, whereupon the θ•T value increases according with the presence of weak ferromagnetic interactions. This behavior was fitted to the Curie-Weiss law with a Weiss constant of χ = +0.2 K. On the contrary, η-phase PTMTC exhibits antiferromagnetic interactions at low temperatures. Indeed, the θ·T value decreases upon decreasing temperature, consistently with the presence of weak intermolecular antiferromagnetic interactions.

-Insert Figure 11 -

Magnetic Property of POROF-2 at Lower Temperatures. The existence of magnetic ordering at very low temperatures was confirmed by variable temperature magnetic susceptibility experiments down to 70 mK and performed in a dilution cryostat. A considerable increase of the θ•T value up to a maximum peak around 110 mK was observed on cooling down below 2 K, which reveals the transition to a ferromagnetic ordered state at very low temperatures. Moreover, the intensity of the peak decreases whereas its maximum shifts slightly to higher temperatures on increasing the external applied magnetic field. For instance, for an applied magnetic field of 20 Oe a value of 2.2 emu·K·mol-1 was obtained, whereas for an external field of 50 Oe the value is reduced to 1.4 emu·K·mol-1. Magnetization curves were measured above and below the critical temperature. Although the magnetization at 1.35 K was dependent linearly on the external magnetic field and therefore the magnetization curve has only a slight

gradient, the curve at 80 mK exhibited a rapid saturation at 400 Oe (Figure 13). It also showed a hysteretic behavior characteristic of a soft ferromagnet, with a coercitive force of the order of 50 Oe.

Conclusions. In conclusion, we designed and prepared perchlorinated triphenylmethyl derivatives carrying carboxylic groups (PTMDC and PTMTC) to form hydrogen-bonded crystals (POROF-1, POROF-2 and η-phase PTMTC). Specifically, POROF-1 and POROF-2 are the first examples of a supramolecular nanoporous paramagnetic pure organic "zeolite-like" material exhibiting an astonishing thermal stability, up to 275 ºC. Among them, POROF-2 exhibits magnetic ordering down to 200 mK, being the first hydrogen-bonded pure organic magnet through carboxylic groups. Furthermore, porosity and magnetic properties can be varied with the introduction of a protic polar solvent in the crystallization process. In such a context, nanoporosity along with the magnetic properties of the such organic frameworks, may open a new avenue to the development of new pure organic multifunctional materials. Further work on this direction is currently underway in our laboratory.

Acknowledgement. This work was supported by the *Programa Nacional de Materiales* of the Dirección General de Investigación (Spain), under project MAGMOL. D.M. is grateful to the Generalitat de Catalunya for a predoctoral grant. D. M. is enrolled in the PhD program of the Universitat Autònoma de Barcelona. We thank to Dr. Xavier Alcobé of the Unitat de Difracció de Raigs-X of Servei CientíficoTècnic of Universitat de Barcelona for X-ray powder diffraction measurements.

Supporting Information Available. This material is available free of charge via the Internet at http://pubs.acs.org.

FIGURES

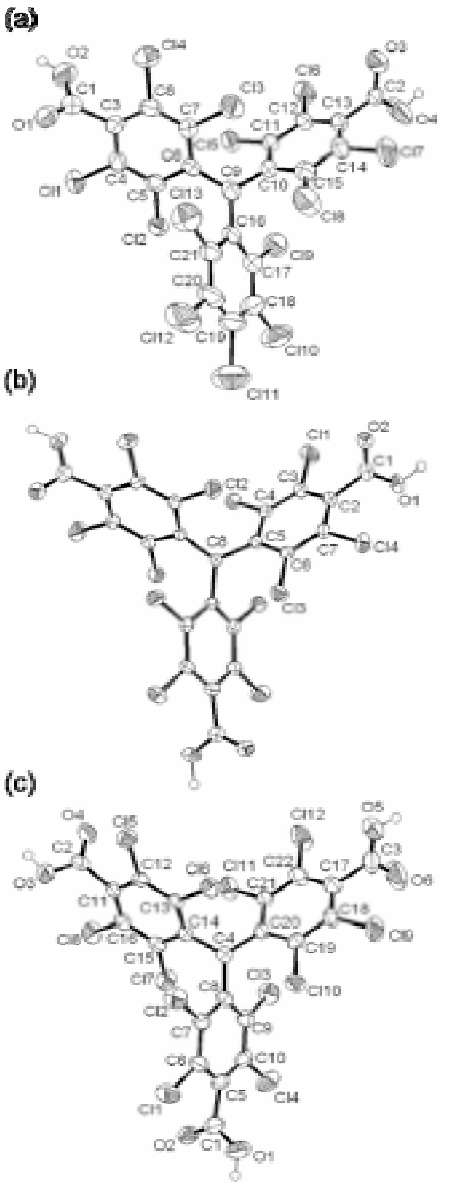

Figure 1. ORTEP plots at 50% of probability of (a) PTMDC in POROF-1, (b) PTMTC in POROF-2, and (c) PTMTC in η-phase.

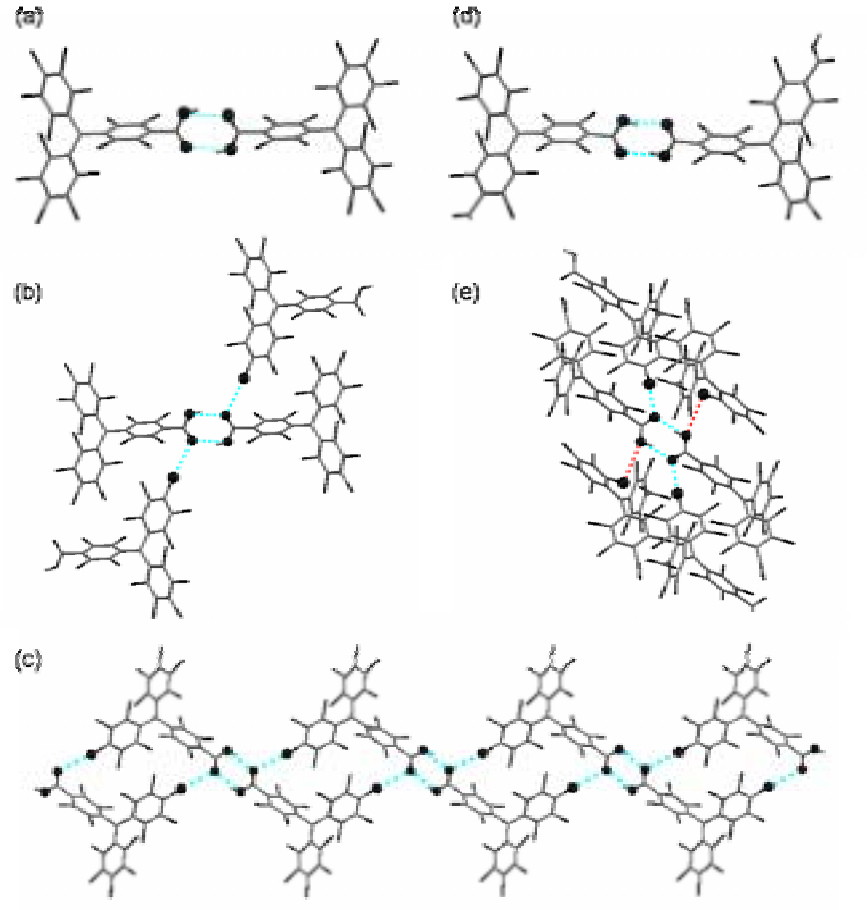

Figure 2. (a) Dimeric motif of PTMMC; (b) bifurcated pattern of PTMMC; (c) hydrogen-bonded chain in PTMMC; (d) dimeric motif of POROF-1; and (e) bifurcated pattern of POROF-1.

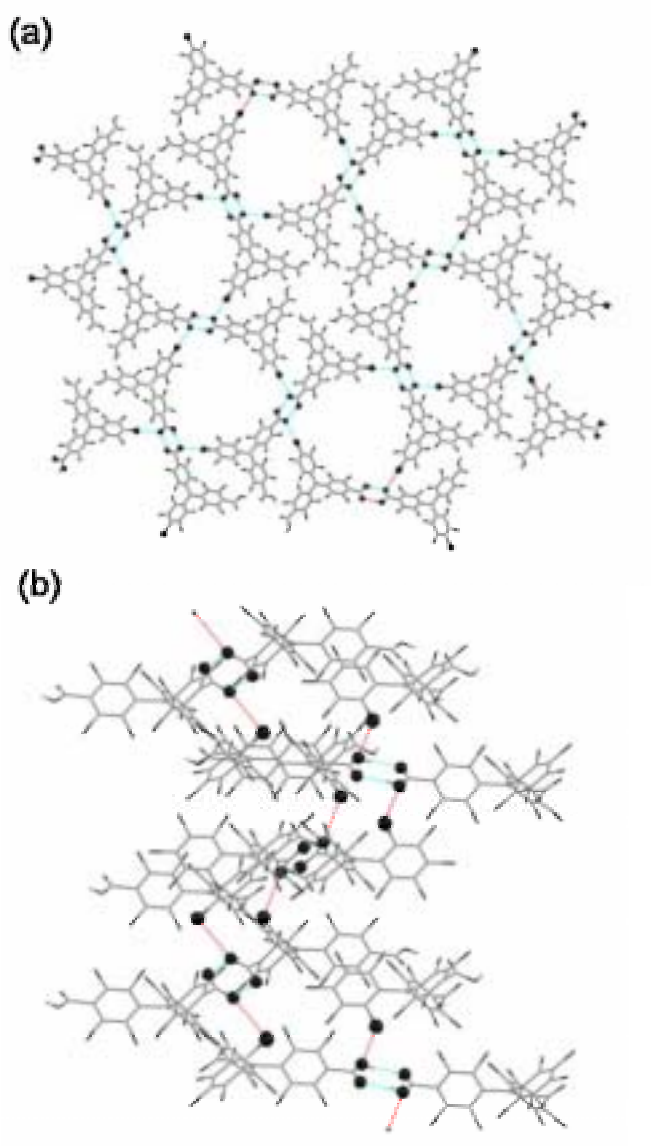

Figure 3. (a) H-bonded plane formed by $R^2_2(8)$ dimers and O3···Cl11 H-bondings along the *ab* plane; (b) H-bonded planes connected through O4···Cl9 H-bondings along the *c* axis.

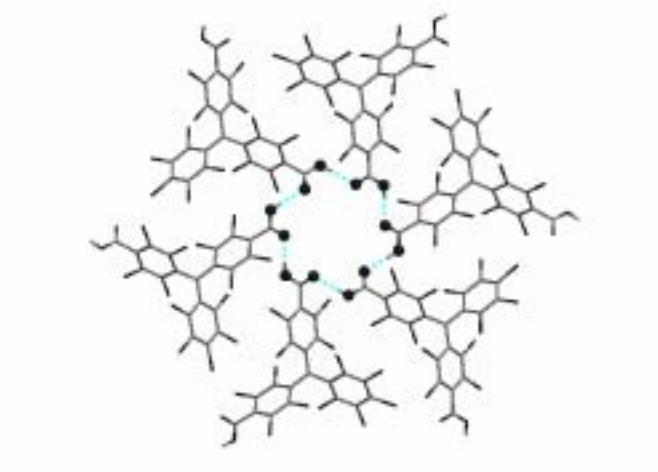

Figure 4. H-bonded hexameric $R^6_6(24)$ motif formed by six PTMDC or PTMTC radicals.

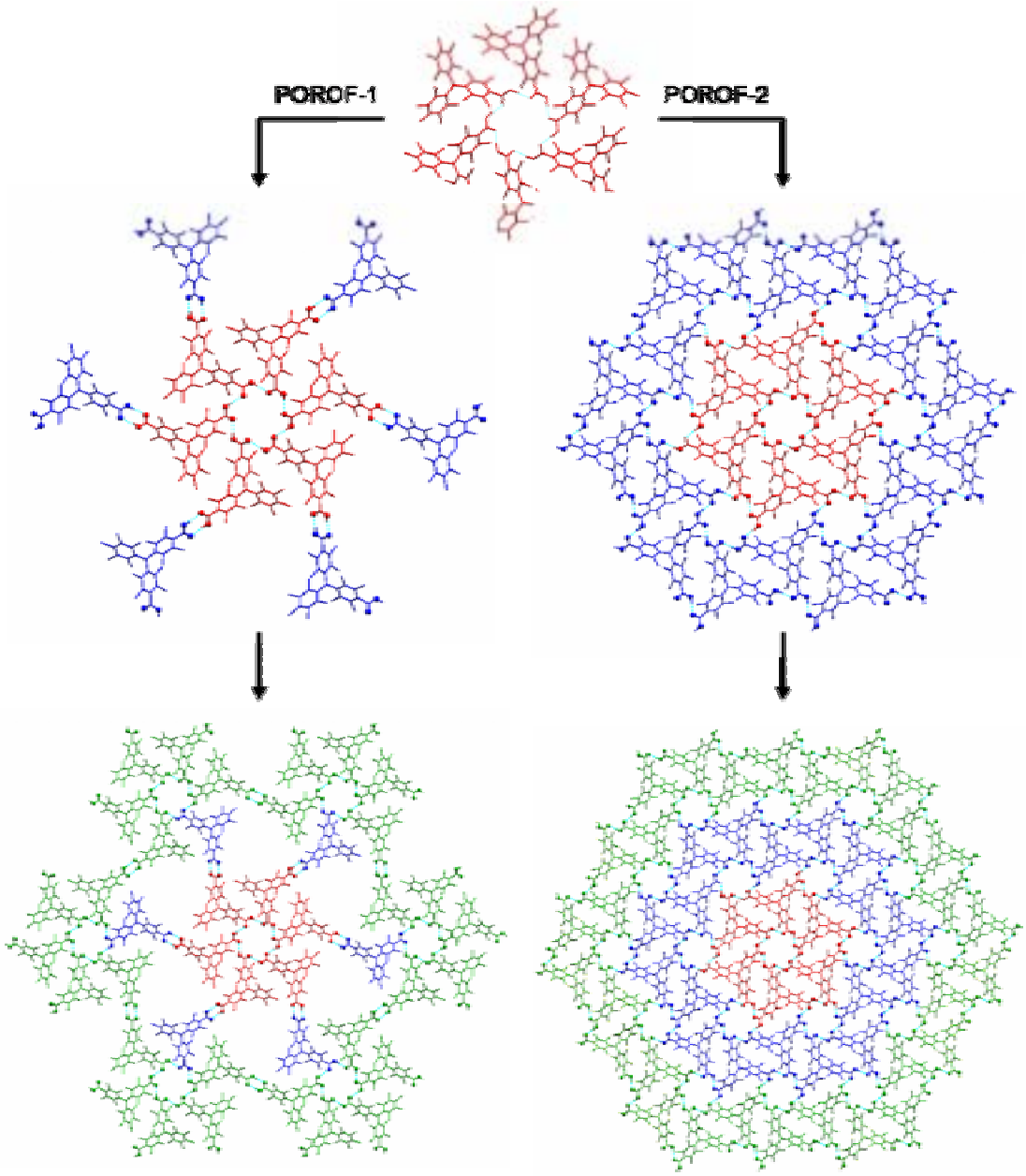

Figure 5. Step-wise growing of the 2-D H-bonded sheets in POROF-1 and POROF-2.